*Physics of the Earth and Planetary Interiors*, 21 (1980) 283–304



# EARTHQUAKE DOUBLETS IN THE SOLOMON ISLANDS

THORNE LAY and HIROO KANAMORI

*Seismological Laboratory, California Institute of Technology, Pasadena, CA 91125 (U.S.A.)*

(Received May 4, 1979; revised and accepted July 5, 1979)

Lay, T. and Kanamori, H., 1980. Earthquake doublets in the Solomon Islands. Phys. Earth Planet. Inter., 21: 283–304.

Large, shallow, thrust earthquakes in the Solomon Islands region tend to occur in closely related pairs. Two recent sequences are July 14, 1971 ($M_S$ = 7.9) and July 26, 1971 ($M_S$ = 7.9) and $14^h37^m$, July 20, 1975 ($M_S$ = 7.9) and $19^h54^m$, July 20, 1975 ($M_S$ = 7.7). The mechanism of these seismic doublets has important bearing on the triggering mechanism of earthquakes in subduction zones. Detailed analysis of the seismic body waves and surface waves were performed on the 1971, 1974, and 1975 doublets, providing a better understanding of: (1) the mechanics of seismic triggering, (2) the state of stress on the fault plane, and (3) the nature of subduction between the Pacific and Indian plates. The results indicate that although the geometry of the subduction zone in the Solomon Islands is complicated by the presence of several sub-plates, the slip direction of the Indian plate with respect to the Pacific plate is relatively uniform over the entire region. The large seismic moments of the 1971 sequence ($1.2 \cdot 10^{28}$ and $1.8 \cdot 10^{28}$ dyne cm) indicate that these events directly represent the underthrusting of the Indian and Solomon plates beneath the Pacific plate. The body waves from these doublets, recorded on the WWSSN long-period seismograms, are remarkably impulsive and simple compared with those from events of comparable seismic moment in other subduction zones. In addition, the source dimensions of the body waves are 30–70 km in length, substantially smaller than the overall rupture surfaces radiating the surface waves which are 100–300 km in length. These facts suggest the existence of relatively large, isolated high-stress zones on the fault plane. This type of stress distribution is distinct from other regions which have more heterogeneous stress distribution on the fault plane, and this is proposed as the principal characteristic of this region responsible for the occurrence of the doublets and for the apparent efficiency of triggering in the Solomon trench. Prior to the 1971 sequence, similar sequences have occurred in the same area in 1919–1920 and 1945–1946. From the amount of slip (1.3 m) determined for the 1971 sequence and the apparent recurrence interval of 25 years, a seismic slip rate of 5 cm $yr^{-1}$ is determined. This value is a significant portion of the convergence rate between the Indian and Pacific plates indicating that the plate motion here is taken up largely by seismic slip.

## 1. Introduction

Large, shallow earthquakes in the Solomon and New Britain Islands region tend to occur in closely related pairs (Figs. 1 and 3). These events are typically separated by a few hours or several days in time and by 50–100 km in space. Although earthquake doublets have been observed in several different tectonic regimes, the Solomon Islands region is apparently unique in having shallow thrust events of such large size ($M_S \geqslant 7.5$) occur in pairs. At least three pairs of events with $M_S \geqslant 7.5$ and several additional doublets with $M_S \geqslant 7.0$ have occurred in distinct portions of the Solomon trench in this decade alone. A search of the earthquake catalogues reveals that this doublet behavior is common for great earthquakes in the area, indicating that this mode of failure is a true characteristic of the region. This paper presents the results of a complete surface-wave and body-wave analysis of three doublets in this region in an attempt to provide a better understanding of the mechanics of seismic triggering, the state of stress on the fault plane, and

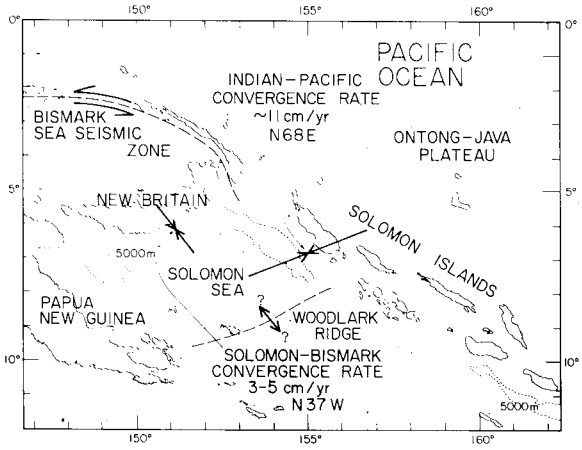


Fig. 1. Principal tectonic features of the Solomon Islands region. The Indian plate underthrusts the Ontong–Java Plateau along the Solomon Islands chain. The 5000 m depth contours indicate the disappearance of the Solomon trench in the vicinity of the Woodlark ridge. The Indian–Pacific convergence rate and direction are from Le Pichon (1968) and Minster et al. (1974). The Solomon–Bismark convergence rate is from this study and Johnson and Molnar (1972).

the nature of subduction between the Pacific and Indian plates.

Much recent effort has been directed toward elaborating the stress distribution on earthquake fault planes. Detailed seismological investigations have revealed a great diversity of focal process of earthquakes, including slow precursory deformation (Kanamori and Cipar, 1974; Nagamune, 1977); long time-constant crustal deformation accompanying tsunami earthquakes (Kanamori, 1972; Fukao and Furumoto, 1975; Shimazaki and Geller, 1977); slow earthquakes (Sacks et al., 1978; Kanamori and Stewart, 1979); and multiple-rupture events (e.g. Wyss and Brune, 1967; Kanamori and Stewart, 1978). This diversity of earthquake process is a manifestation of the diversity of stress distribution on fault planes and of variable coupling between lithospheres. The distinct doublet nature of earthquakes in the Solomon Islands region provides further information on the nature of lithospheric coupling.

As is frequently the case for South Pacific thrust events, the focal mechanisms determined from first-motion data alone are ambiguous, usually constraining at most one nodal plane. In this study we sought to extract as much information as possible about the source parameters of the sequences by using long-period surface waves and, whenever possible, body waves. The detailed signal analysis employed provides unambiguous fault plane parameters, seismic moments, displacements, and stress drops of the individual events. The information thus extracted is supplemented by previous seismicity studies of the region in order to construct a plausible model for the tectonic framework and nature of coupling in the subduction zone. Previous seismicity studies have indicated the general geometry of the trench system (Denham, 1969; Santo, 1970; Isacks and Molnar, 1971; Johnson and Molnar, 1972; Curtis, 1973a, b; Pascal, 1979), but this paper presents the first quantitative analysis of particular events in the region, allowing improved constraints to be placed on the nature of subduction there.

## 2. Tectonic framework

Figure 1 locates the Solomon Islands region east of New Guinea, in the complex mega-shear boundary between the Pacific and Indian plates. The complexity of this boundary apparently stems from collision in Miocene times of the northward-moving Indian plate with a large, southward-facing island arc (Dewey and Bird, 1970; Karig, 1972). Regional adjustment to this event has produced several small plates and island arc reversals as well as the "fractured arc" nature of the Solomon Islands chain (Johnson and Molnar, 1972; Curtis, 1973b; Packham 1973). Relevant geologic background is reviewed by Curtis (1973a) and by Coleman and Packham (1976). In Fig. 1 it is clear from the 5000 m depth contours that the trench has an unusual geometry. The results of this work and previous seismicity studies indicate that along the Solomon Islands the Solomon Sea slab subducts toward the northeast in the Solomon trench, while under New Britain the subduction is toward the northwest. Thus, the slab is contorted around the junction of the Solomon and New Britain trenches. Toward the northeast lies the Ontong–Java Plateau which has a thick (35–40 km) semi-continental crustal structure (Furumoto et al., 1976). The trench along the Solomon Islands chain disappears in the vicinity of the Woodlark Ridge, and reappears down toward the southeastern end of the chain. Clearly,

there are substantial variations in the subduction regime over small distances in this region. A more detailed discussion of the tectonics will follow the doublet analysis.

## 3. Data

Figure 2 shows the Pasadena ultra-long period seismogram of a Solomon Islands doublet which occurred in 1974. This vertical component seismogram records the multiple Rayleigh-wave arrivals from the two events, which are separated by less than four hours in time. This record demonstrates the intriguing nature of these sequences, occurring as distinct similar events, which led to this investigation. Three doublet sequences have been studied, all located in the northwestern portion of the Solomon trench and extending into the New Britain trench. The locations of these events and their two-day aftershock zones are plotted in Fig. 3. The focal mechanisms shown in the Figure have been determined by the surface wave analysis described in the next section since the P-wave first-motion mechanisms are very poorly constrained. The first-motion data are included with the mechanisms and show very little inconsistency with the surface wave results. All of the first-motions were read by the authors from the World-Wide Standard Seismograph Network (WWSSN) long-period seismograms. Of the six events, two, those of the 1971 sequence, had first-motion mechanisms previously published by Pascal (1978), both of which differ substantially from our solutions which are better constrained by surface waves.

The 1971 sequence was composed of the largest events in the region in 50 years. It occurred at the junction of the two trenches, with the first event in the Solomon trench triggering the rupture in the New Britain trench. The 1974 and 1975 sequences occurred in the Solomon trench along the island of Bougainville. The times, locations, and magnitudes of these events given in the Earthquake Data Reports (EDR) are listed in Table I. The values of $M_S$ vary in different catalogues, but the only significant variations are for the 1975 sequence, for which Pasadena reports $M_S = 7.8$ and $M_S = 7.3$ for the first and second events respectively and Berkeley reports $M_S = 7.4$ and $M_S = 7.3$.

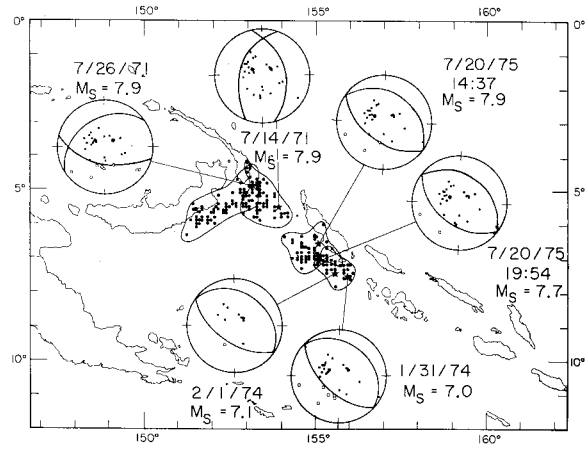


Fig. 3. The three doublets analyzed in this work. The first-motion data are shown along with the surface wave constrained fault orientations on equal area projections of the lower half of the focal sphere, with filled circles indicating compression and open circles indicating dilatation. Two-day aftershock zones are also shown for aftershocks of $m_b \geq 4.5$.

The aftershock locations shown in Fig. 3 are taken from the EDR and the Bulletin of the International Seismological Centre (ISC) catalogues, and only the larger ($m_b \geq 4.5$), better located events are included. Note the similarity of the 1974 and 1975 doublet

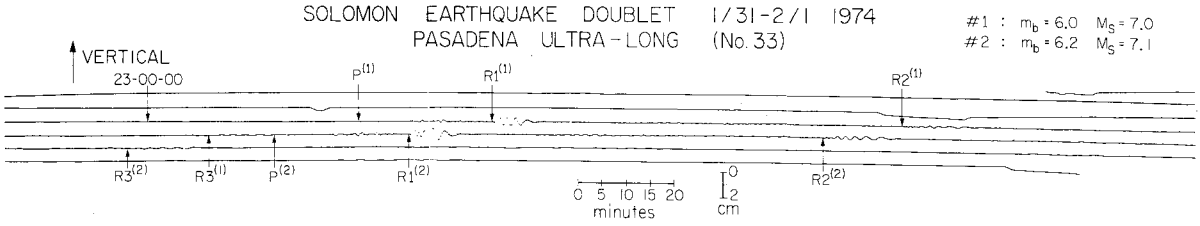


Fig. 2. The Pasadena ultra-long period seismogram of a Solomon Islands doublet which occurred in 1974. This vertical component records the multiple Rayleigh wave arrivals $R_1$, $R_2$ and $R_3$, for each event. The two events are separated by $3^h42^m$.

TABLE I

Earthquake data

| Event | Origin time (UT) | Lat. (°S) | Long. (°E) | $m_b$ | $M_s$ |
|---|---|---|---|---|---|
| July 14, 1971 | 06 : 11 : 29.1 | 5.5 | 153.9 | 6.0 | 7.9 |
| July 26, 1971 | 01 : 23 : 21.3 | 4.9 | 153.2 | 6.3 | 7.9 |
| Jan. 31, 1974 | 23 : 30 : 05.3 | 7.5 | 155.9 | 6.0 | 7.0 |
| Feb. 01, 1971 | 03 : 12 : 33.1 | 7.8 | 155.6 | 6.2 | 7.1 |
| July 20, 1975 | 14 : 37 : 39.9 | 6.6 | 155.1 | 6.6 | 7.9 |
| July 20, 1975 | 19 : 54 : 27.7 | 7.1 | 155.2 | 6.1 | 7.7 |

mechanisms, and the fact that the aftershock zone dimensions are on the order of 100–150 km in length and ~75–100 km in width. Since the main shocks of the 1974 and 1975 doublets were separated by only $3^h42^m26^s$ and $5^h16^m49^s$ respectively, no attempt is made in Fig. 3 to delineate separate aftershock zones of the individual events. There were three events of magnitudes $m_b = 4.8$–$5.2$ recorded between the two main events of the 1974 sequence, and 19 events of $m_b = 4.5$–$5.5$ recorded between the main events of the 1975 sequence. In each sequence the second large event is well-separated from the first, the separation being about 50 km as given by catalogue locations and as confirmed by the authors through comparison of azimuthal travel-time variations. The 1971 sequence was separated by 12 days, and thus the aftershock zones are distinct. The aftershock activity following the first event on July 14 migrated northwest along the Solomon trench and concentrated along the bathymetric junction of the trenches. The July 26 event had an epicenter at this junction and its aftershocks were confined to and propagated southwest down the New Britain trench. Note the presence of a gap between the 1971 and 1975 sequences. Seismicity studies show a persistent low seismic activity in this region (Curtis, 1973a).

Of the three sequences studied, only the smaller 1974 doublet had local foreshocks, there being two of these of magnitudes $m_b = 5.3$ and $m_b = 4.8$, preceding the first main-shock by $3^h14^m$ and $1^h23^m$ respectively. Aftershock activity was relatively low and tapered off rapidly within 48 hours for each sequence except the 1971 doublet, when events continued to occur for a substantially longer time-period in the New Britain trench. The July 14, 1971 event had 27 aftershocks listed in the ISC catalogue with $m_b \geqslant 4.5$ in the first 24 hours after the main event, while there were 24 aftershocks following the 1974 sequence and 28 following the 1975 sequence in the same 24 hour interval. Activity then leveled off to several events per day in each case. The July 26, 1971 event was immediately followed by 43 aftershocks on the first day and 37 on the second day, with activity dropping off substantially slower than in other cases. This discrepancy is associated with the larger size of the July 26 event, but may also indicate a difference in mechanical coupling between the Solomon and New Britain trenches. Due to its location, the detection threshold for the Solomon Islands is relatively high, but the observed seismicity patterns are considered representative since they include only events with $m_b \geqslant 4.5$.

The 1971 and 1975 sequences were large enough to drive off-scale most of the WWSSN long-period body wave arrivals. Thus, we chose to determine the earthquake mechanisms primarily by surface-wave analysis. Figures 4, 5, 7, 8, 10, 11 show the surface waves that were recorded by the WWSSN long-period seismographs. In Figs. 4 and 5 the data for the 1971 sequence is shown. Here Love waves ($G_3$) and Rayleigh waves ($R_3$) have been equalized to a propagation distance of 360° + 90°, following the technique described by Kanamori (1970). The equalized traces have been filtered using a short period cut-off at 40 s in the same manner as described by Kanamori and Stewart (1976), and the amplitudes have been adjusted to the standard WWSSN (15–100) instrument with a gain of 1500. Figures 7 and 8 present the data for the 1974 doublet and Figs. 10 and 11 present the data for the 1975 events. For these last two doublets, surface waves $R_2$ and $G_2$ were equal-

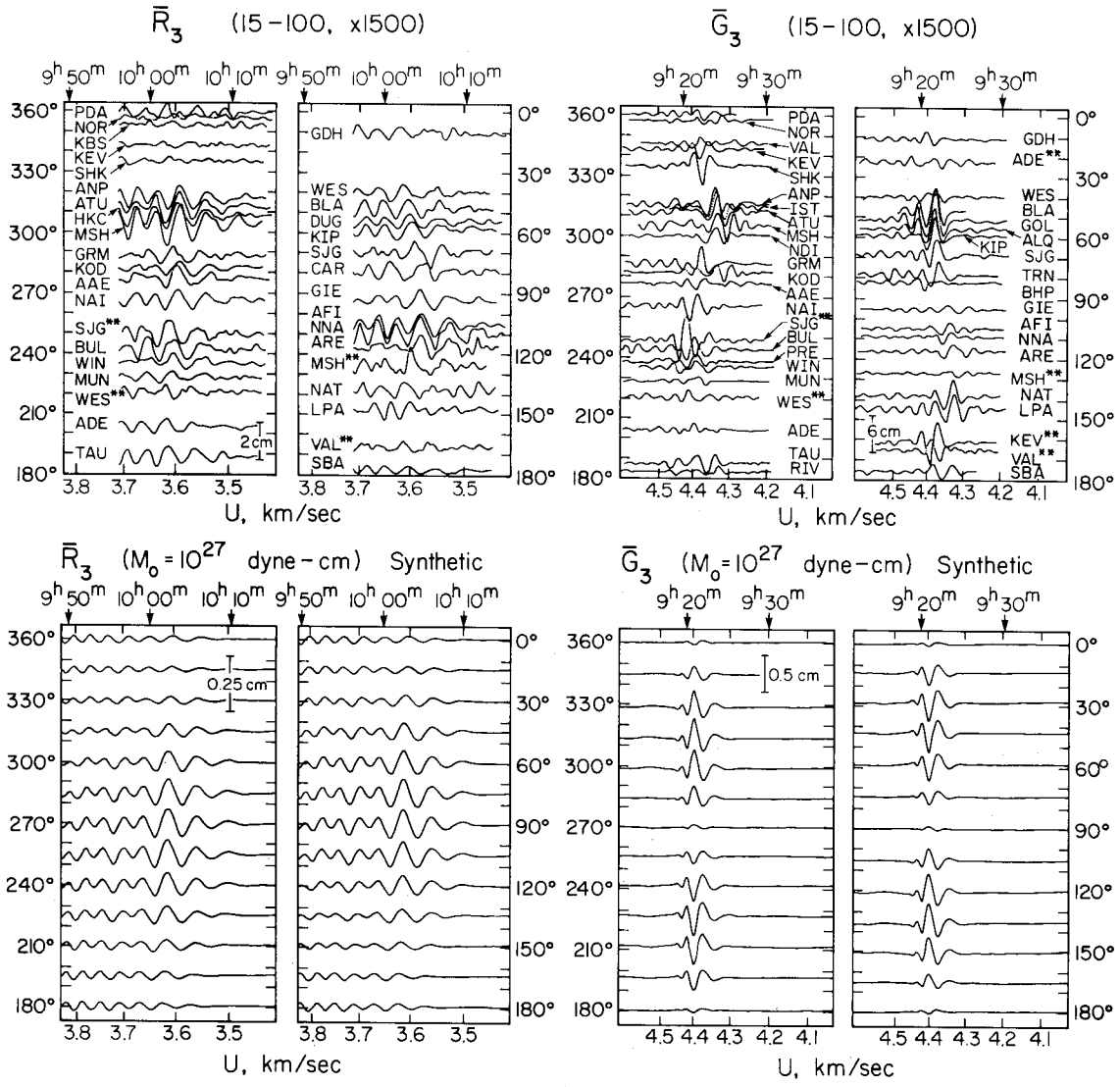


Fig. 4. Equalized seismograms of $G_3$ and $R_3$ for the July 14, 1971 event and synthetic seismograms computed for the mechanism given in Table II with a seismic moment of $10^{27}$ dyne cm. Two asterisks represent $G_4$ and $R_4$ arrivals equalized to $G_3$ and $R_3$. The amplitude scale is for the trace amplitude on the WWSSN long-period instrument (15–100) with a magnification of 1500.

ized to propagation distances of 270°. These surface wave arrivals were employed because the main events were not separated by enough time to obtain all $R_3$ arrivals. In order to extend the azimuthal coverage, where necessary, the data was supplemented with backward-propagated $R_4$, $G_4$, or $R_3$, $G_3$ and forward-propagated $R_1$, $G_1$ arrivals. This allowed for better constraint of the mechanisms. In all cases the Rayleigh waves exhibit two-lobed radiation patterns and the Love waves exhibit four-lobed radiation patterns as is consistent with shallow dipping thrust events (Kanamori, 1970). This extensive data set constitutes the basic information employed in this analysis, and represents one of the most self-consistent surface wave data sets of any particular tectonic region. The following two sections contain detailed descrip-

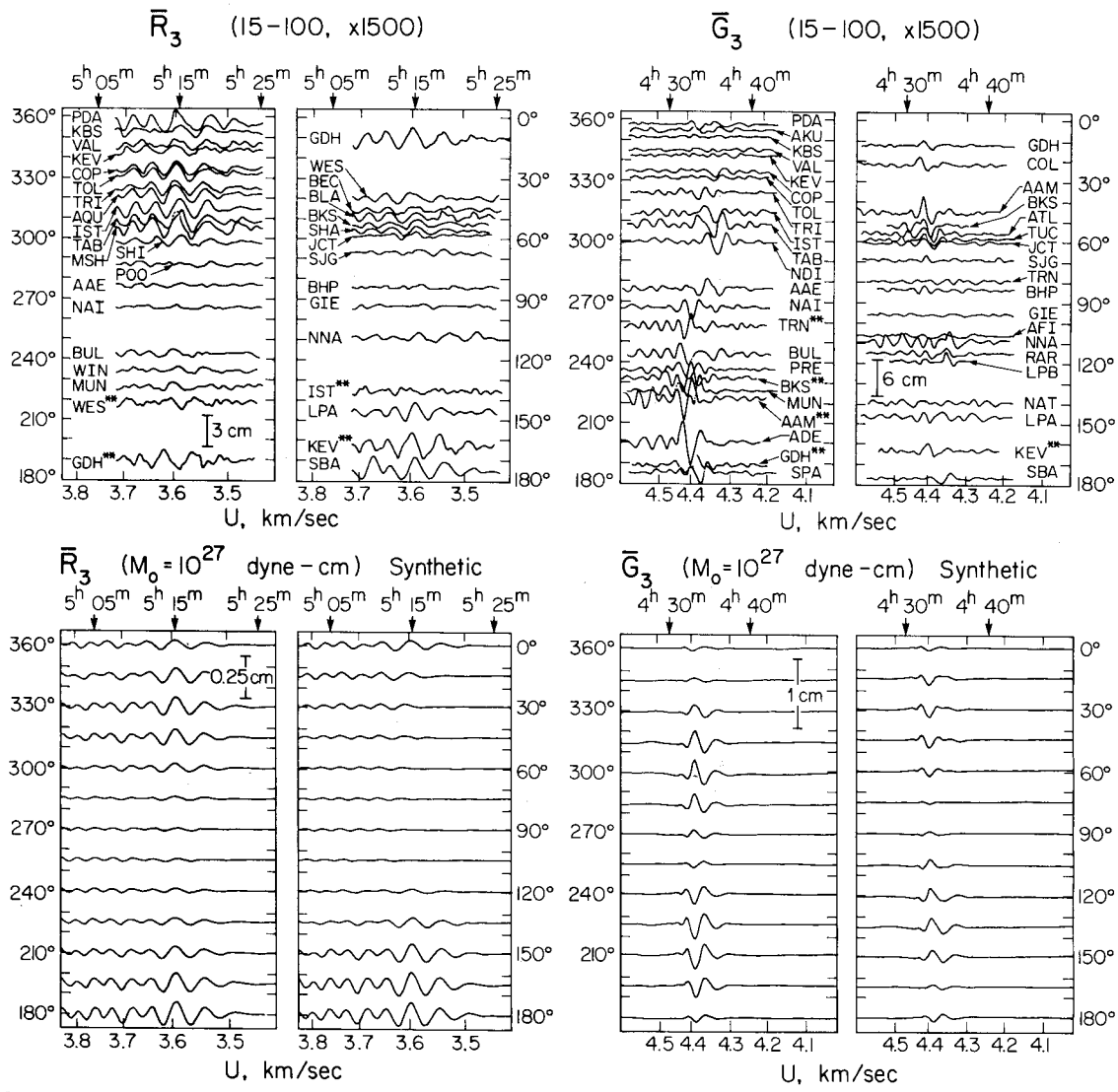


Fig. 5. Equalized seismograms of $G_3$ and $R_3$ for the July 26, 1971 event, and synthetic seismograms for the finite source discussed in the text.

tions of the surface wave and body wave analysis. The tectonic framework and doublet mechanism are discussed in Sections 6 and 7.

## 4. Surface-wave analysis

### *4.1. 1971 Sequence*

The two events in this sequence proved to have slightly more complicated structure in their radiation patterns than the other events. This is attributed to both their larger seismic moments and fault dimensions and to their location at the trench junction. Utilizing the best initial mechanisms indicated by our first-motion data and the previously published mechanisms, synthetic surface waves were generated for a point source double-couple. It was found that preliminary inspection of the equalized-trace azimuthal amplitude variations proved a better constraint for the initial modelling than the first-motion results. The procedure employed for generating the synthetics is

exactly that described by Kanamori (1970) and Kanamori and Cipar (1974) with Earth model 5.08 *M* being used. As with the observed data, a 40 s cut-off filter was applied to the synthetics enabling direct comparison of phases and amplitudes. The amplitudes used for constraining the mechanism are those of the Rayleigh waves with a period of about 220 s and the peak amplitudes of the less-dispersed Love wave arrivals. These long-period waves are much less sensitive to propagational effects and lateral heterogeneity than shorter period phases. The ratio of peak amplitudes of Love and Rayleigh waves also provides a strong depth constraint, though the depths indicated by this technique must be considered as averaging over the fault surface, and do not necessarily correspond to the depths determined from the body-wave analysis.

The July 14, 1971 event (Figs. 4 and 6) has rather more scatter in amplitudes than any of the other five events, but it could still be satisfactorily modelled. The source depth was found to be 53 km. A seismic moment of $1.2 \cdot 10^{28}$ dyne cm gives a reasonably good fit to the data with the fault parameters being dip, $\delta = 45°$; rake, $\lambda = 62°$; and strike, $\phi = 345°$. In this, and all five other events, the choice of fault plane between the two nodal planes is made on the basis of consistency with the regional tectonics and the interpretation of these as shallow thrust events. The sign conventions are those of Kanamori and Cipar (1974). The azimuthal distribution of wave forms for this mechanism is given in Fig. 4 and the amplitude variation is plotted with the data in Fig. 6. There is some asymmetry in the Love wave radiation pattern, with signals in the southwest quadrant being somewhat smaller than the model. The cause of this is not readily apparent, and since the point source fit to the other Love wave lobes and Rayleigh wave pattern is good, we attribute this anomaly to the scatter which frequently accompanies Love wave amplitudes.

Note the generally excellent phase agreement observed in the data for this and the other events. This consistency indicates that great circle travel paths through the Solomon Islands traverse relatively similar average paths. As a result of this consistency the phase agreement with the longer periods of the synthetics is very good, though the Love waves are not as stable as the Rayleigh waves. One consistent pattern observed in the Love waves between events is

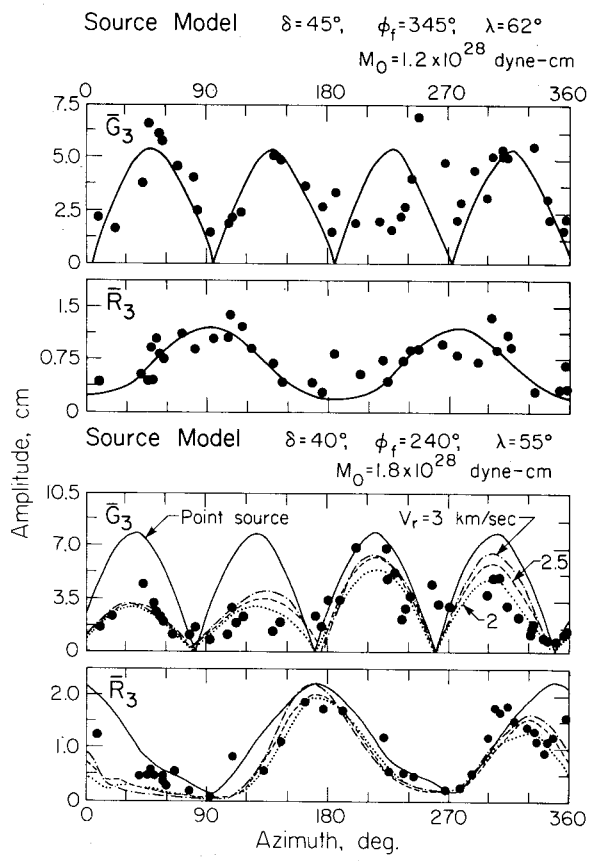


Fig. 6. Equalized trace peak-to-peak amplitudes for observed $G_3$ and $R_3$ data as a function of azimuth (solid circles) for the July 14, 1971 (top) and the July 26, 1971 events. Curves represent the radiation patterns for the given fault models.

that the group arrivals tend to be slightly delayed in the northwestern quadrant which includes the Asian and European continents.

This event appears somewhat unusual with regard to the strike of the fault plane (Fig. 3), which trends more north–south than the other mechanisms. Detailed examination of the bathymetry in the epicentral region indicates that the trench tends to strike slightly more northward along Bougainville, and thus the fault strike of 340°, one of the fault parameters best determined by this type of analysis, is consistent with the trench geometry.

The second 1971 event definitely has an asymmetric radiation pattern, and the fault plane clearly lies in the New Britain trench trending northeast–southwest (Fig. 5), as indicated by the loop directions of the

Rayleigh waves. Figure 6 shows the radiation pattern for a point source located at the body wave epicenter at a depth of 43 km with $\delta = 40°, \lambda = 55°, \phi = 240°$, and a moment of $1.8 \cdot 10^{28}$ dyne cm. Clearly the eastern lobes of the Love wave radiation pattern are consistently smaller than the western lobes. In order to improve the fit we generated synthetics incorporating the effects of directivity (Ben-Menahem, 1961). As indicated in Fig. 3 the aftershock zone of this event extends well down the New Britain trench, with a total length of 300 km. Using the geometry of the point source we attempted various directivity models constraining the total fault length to be 300 km. The most consistent results were those for a bilateral fault with a northeastern length of 100 km and a southwestern length of 200 km, with rupture propagating along the strike, $\phi = 240°$. The amplitude radiation patterns for this fault model for varying rupture

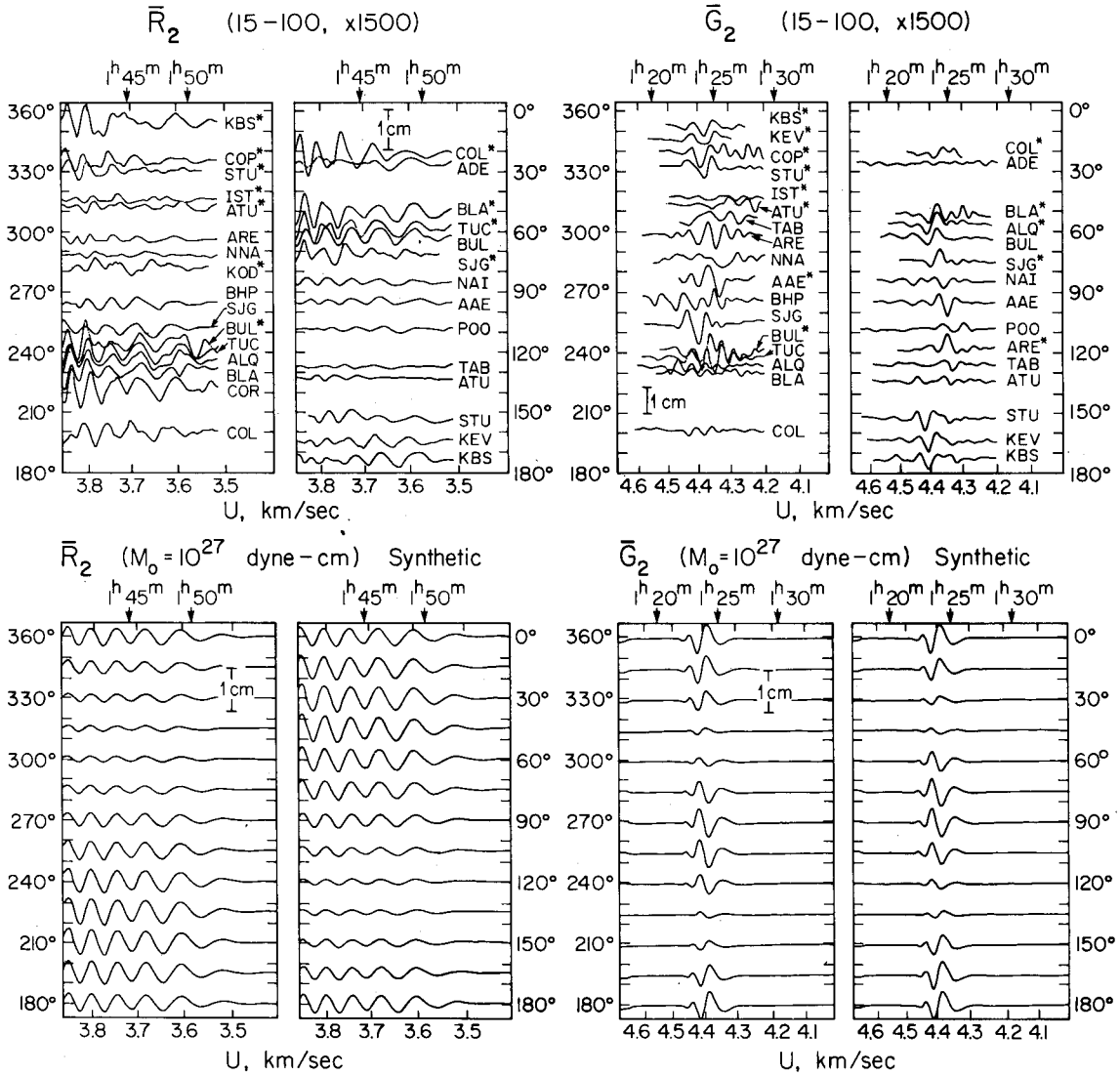


Fig. 7. Equalized seismograms of $G_2$ and $R_2$ for the Jan. 31, 1974 event and synthetic seismograms computed for the mechanism given in Table II. In this and the following figures two asterisks represent $G_3$ and $R_3$ data equalized to $G_2$ and $R_2$, and single asterisks represent $G_1$ and $R_1$ data equalized to $G_2$ and $R_2$.

velocities are shown in Fig. 6, for a moment of $1.8 \cdot 10^{28}$ dyne cm. Given the slight scatter around each model we conclude that rupture velocities of $V_r = 2.0$ km s$^{-1}$ or $V_r = 2.5$ km s$^{-1}$ are most reasonable. The synthetic wave forms for $V_r = 2.5$ km s$^{-1}$ are plotted in Fig. 5 for comparison with the data. This procedure incorporates the assumption of uniform dislocation along the fault strike which appears justified by the quality of the match obtained.

This 1971 doublet is the most significant sequence studied because the two events involved are the largest in the region since 1919 and they occurred at the trench junction. The fault mechanisms obtained by the surface wave analysis are much better constrained than the first-motion mechanisms. Indeed, there was enough ambiguity in the first-motion data that earlier work (Pascal, 1979) located the thrust plane of the July 26 event in the Solomon trench rather than in the New Britain trench.

Given the seismic moment and a reasonable estimate of the fault area $A$ as indicated by immediate

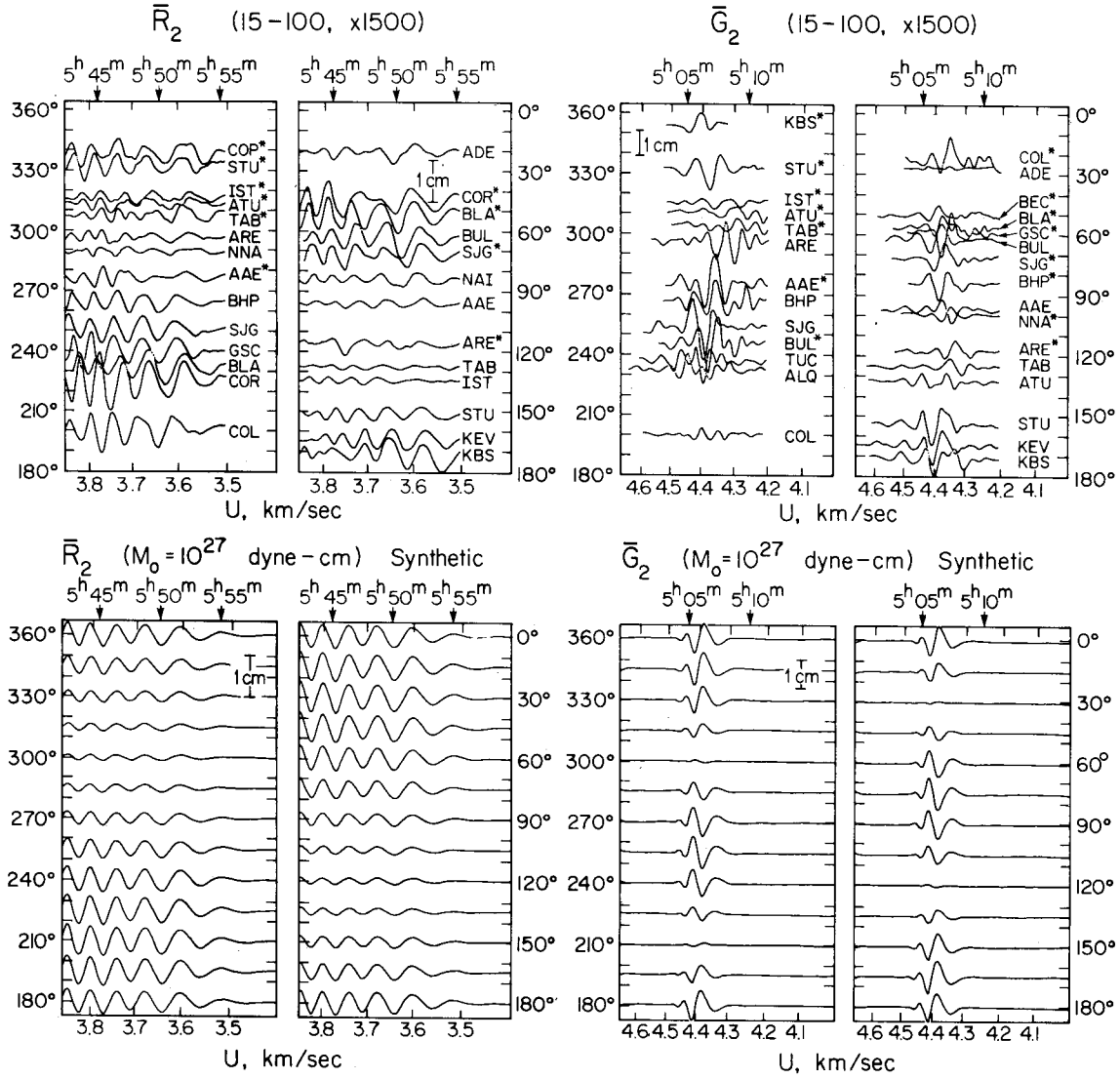


Fig. 8. Equalized seismograms of $G_2$ and $R_2$ for the Feb. 1, 1974 event and synthetic seismograms.

aftershock locations, one can obtain values for the average dislocation $\bar{D}$ and the stress drop $\Delta\sigma$. We noted that since tsunami accompanied all of the events studied we could assume that the fault plane extended to the surface. For the July 14 event we found $\bar{D} = M_o/\mu A = 1.3$ m and $\Delta\sigma = 7\pi^{3/2}\mu\bar{D}\,A^{-1/2}/16 = 19$ bar, using $\mu = 7 \cdot 10^{11}$ dyne cm$^2$. For the July 26 event $\bar{D} = 1.3$ m and $\Delta\sigma = 17$ bar.

### *4.2. 1974 Sequence*

The 1974 sequence is less complicated and quite a bit smaller than the 1971 doublet. The epicenters are both located in the Solomon trench and the observed radiation patterns are very similar for both events (Figs. 7 and 8). The ratios of Love wave to Rayleigh wave amplitudes indicate a source depth of 16 km, substantially less than for the 1971 events and consistent with the apparent shallowing of the trench bathymetry and regional seismicity toward the central Solomon Islands (Denham, 1969). Again, the data demonstrate consistent phase agreement and less scatter in amplitudes. In Fig. 9 we show the azimuthal amplitude variations of the data and synthetics. There is no strong indication of directivity and the orientation of loop and node directions of the radiation patterns do not indicate any resolvable rake variations from pure thrust. The Rayleigh wave radiation patterns are particularly consistent with pure thrust.

The January 31, 1974 event was found to be well-fit with a source mechanism of $\delta = 28°$, $\phi = 309°$, $\lambda = 90°$, and a seismic moment of $1.0 \cdot 10^{27}$ dyne cm. The February 1 event has a source mechanism of $\delta = 34°$, $\phi = 302°$, $\lambda = 90°$, with a seismic moment of $1.4 \cdot 10^{27}$ dyne cm. The wave-form and amplitude variations for these synthetic models are shown in Figs. 7, 8, 9. The quality of the data is considered to be good enough to definitely resolve the slight differences in these mechanisms. In each pattern there are some slightly enhanced Love wave amplitudes in the southwestern quadrant (Fig. 9) suggestive of some up-dip propagation, but given the usual scatter observed in Love wave amplitudes and the small aftershock area of these events finite source models were not investigated.

The displacements and stress drops for this doublet were determined by summing the moments of the individual events and by using the total area of the aftershock zone. This was done because the individual fault dimensions are not resolvable. This procedure yields $\bar{D} = 0.6$ m and $\Delta\sigma = 12$ bar. These values are appropriate estimates for each of the events since they occurred close together in time and space on the same fault plane.

### *4.3. 1975 Sequence*

The July 20, 1975 doublet is of intermediate size, but most nearly resembles the 1974 doublet in the similarity of its radiation patterns. The doublet occurred along Bougainville Island and its aftershock zone only slightly overlaps the zone of the 1974 doublet, and the mechanisms are very similar. Figures 10

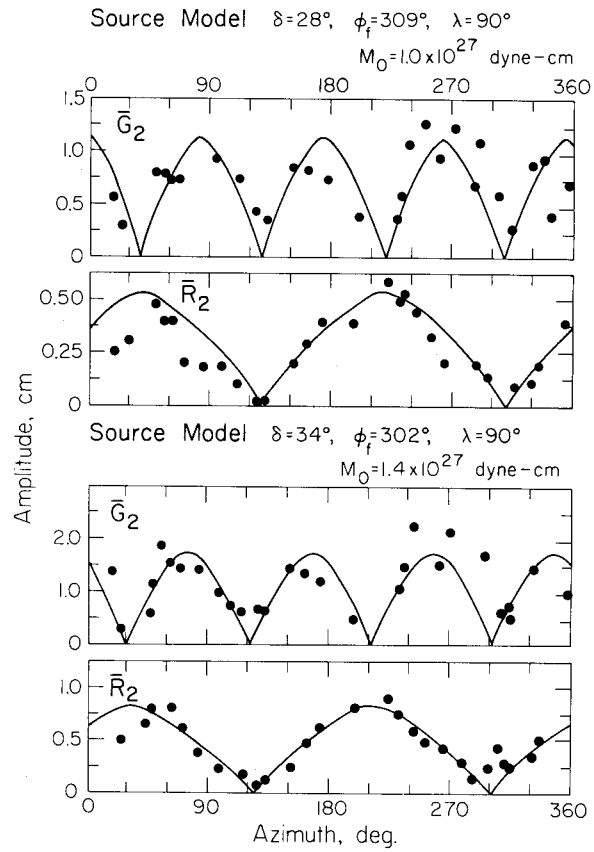


Fig. 9. Peak-to-peak amplitudes of the equalized data and fault models versus azimuth for the Jan. 31, 1974 (top) and Feb. 1, 1974 events.

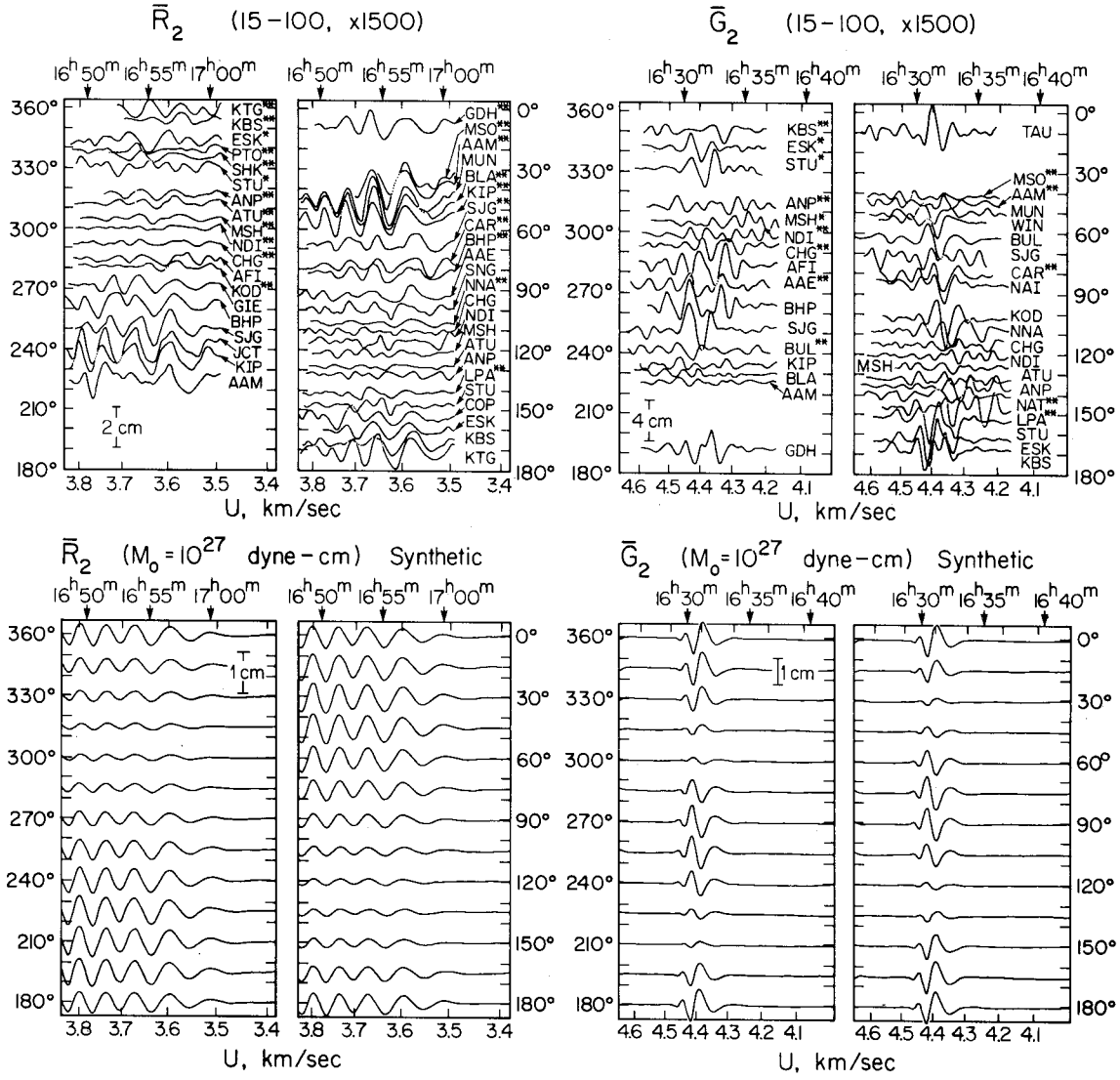


Fig. 10. Equalized seismograms of $G_2$ and $R_2$ for the $14^h37^m$ July 20, 1975 event and synthetic seismograms.

and 11 show the equalized data sets and synthetics generated in the modelling. Again, the data set, which is very extensive for this doublet, proved most consistent with pure thrust mechanisms.

The $14^h37^m$ event was larger than the accompanying event. Figure 12 shows the amplitude variation for the data and a model with a source depth of 16 km, fault orientation $\delta = 36°$, $\phi = 306°$, and $\lambda = 90°$, and a seismic moment $M_o = 3.4 \cdot 10^{27}$ dyne cm. The $19^h54^m$ event was well modelled with a source depth of 33 km and a fault mechanism of $\delta = 40°$, $\phi = 303°$, $\lambda = 90°$, and $M_o = 1.2 \cdot 10^{27}$ dyne cm. These mechanisms are quite well constrained. It will be seen that the difference in size of these events is also reflected in the body wave complexity. The same method used for the 1974 doublet was employed to calculate $\bar{D}$ and $\Delta\sigma$. For the 1975 events we find $\bar{D} = 0.5$ m and $\Delta\sigma = 9$ bars.

The fault parameters determined from this surface wave analysis are summarized in Table II.

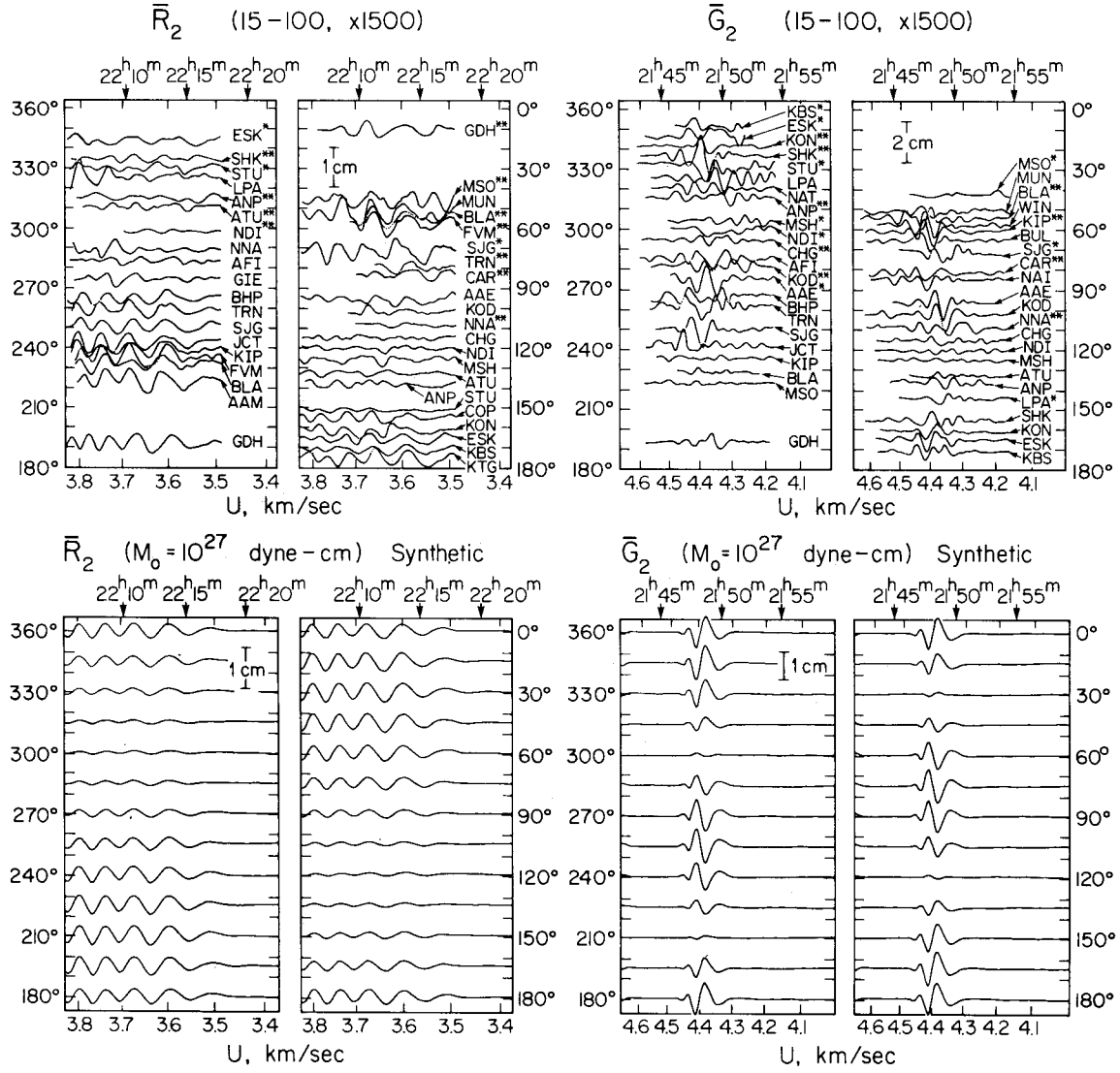


Fig. 11. Equalized seismograms of $G_2$ and $R_2$ for the $19^h54^m$ July 20, 1975 event and synthetic seismograms.

TABLE II

Fault parameters

| Event | $M_s$ | $M_o$ ($10^{27}$ dyne cm) | Strike (°) | Dip (°) | Rake (°) | $D$ (cm) | $\Delta\sigma$ (bar) | $\tau$ (sec) | $t_c$ (sec) |
|---|---|---|---|---|---|---|---|---|---|
| July 14, 1971 | 7.9 | 12.0 | 345 | 45 | 62 | 130 | 19 | 5 | 9 |
| July 26, 1971 | 7.9 | 18.0 | 240 | 40 | 55 | 130 | 17 | 5 | 11 |
| Jan. 31, 1974 | 7.0 | 1.0 | 309 | 28 | 90 | 60 | 12 | – | – |
| Feb. 01, 1974 | 7.1 | 1.4 | 302 | 34 | 90 | 60 | 12 | – | – |
| July 20, 1975 | 7.9 | 3.4 | 306 | 36 | 90 | 50 | 9 | – | – |
| July 20, 1975 | 7.7 | 1.2 | 303 | 40 | 90 | 50 | 9 | 4 | 6 |

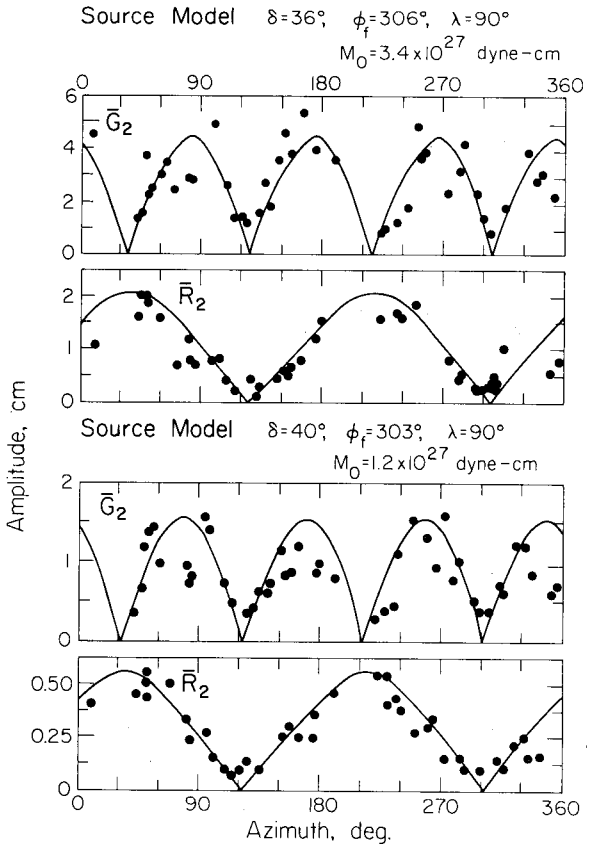


Fig. 12. Peak-to-peak amplitudes of the equalized data and fault models versus azimuth for the July 20, 1975 sequence: $14^h37^m$ (top) and $19^h54^m$.

## 5. Body wave analysis

The 1971 and 1975 doublets were such large events that the on-scale body wave data are of very limited quantity. For example, the July 26, 1971 P-wave is off-scale or ambiguous on all WWSSN vertical seismograms, and the azimuthal coverage for the other large events is scant and tends to be biased toward distances greater than 80°. The 1974 doublet body wave data set is more complete. From the body waves that are on-scale, supplemented with the records of the Pasadena Press–Ewing (30–90) instrument, it appears that the P-waves from the Solomon Islands earthquakes are of unusually impulsive and relatively simple character. Figure 13 shows a sampling of loop direction P-waves and the first few minutes of coda for each of the Solomon Islands events and for events of comparable moment from subduction zones around the Pacific. Through such comparisons we found that two characteristics distinguish the Solomon Islands events; (1) the principal features of the P-wave pulse indicate only one or two distinct ruptures unlike the more common multiple rupture subduction zone events, and (2) the P-waves are very impulsive indicative of abrupt high stress drop failure. In order to assess these observations more quantitatively we sought to bound the P-wave time functions for the 1971 and 1975 events.

The method employed was to generate synthetics following the procedure described in Langston and Helmberger (1975) and Kanamori and Stewart (1976), which gives expressions for the far field P-wave seismogram. This procedure is applied to a trapezoidal moment rate function

$$M(t) = M_0\, T(t; \tau, t_c) \tag{1}$$

where $M_0 = \mu \bar{D} A$. Figure 14 shows the sensitivity of this procedure for bounding the values of rise time $\tau$ and rupture time $t_c$. The *P*-wave observed at GSC from the July 14, 1971 event is compared with synthetics generated for various combinations of $\tau$ and $t_c$. It is clear that the rupture time $t_c$ can be determined with an accuracy of ±2 s, especially if there are several records. This assumes that at least a good approximation of the fault mechanism is known. The motivation for obtaining the rupture time, $t_c$, is that for this simple modelling we can use the approximation $t_c \sim L/V_r$ to estimate the fault length, $L$, where $V_r$ is the rupture velocity. For bilateral faulting $t_c \sim L/2V_r$.

Given that the limited body wave data set in itself was inadequate to constrain the fault parameters we employed the surface wave mechanisms in the first attempts at generating synthetics. The body wave pulse is comprised of interacting P, pP, and sP arrivals, thus the wave form is very sensitive to fault orientation. For all six events the surface wave mechanisms proved consistent with the observed body wave polarities and wave forms.

Body waves and synthetics for the July 14, 1971 event are shown in Fig. 15. The source mechanism differs from that for the surface waves only in that a rake of 90° was used as this slightly improved the wave forms, and the depth of the point source is 37 km. The time function is a symmetric trapezoid with

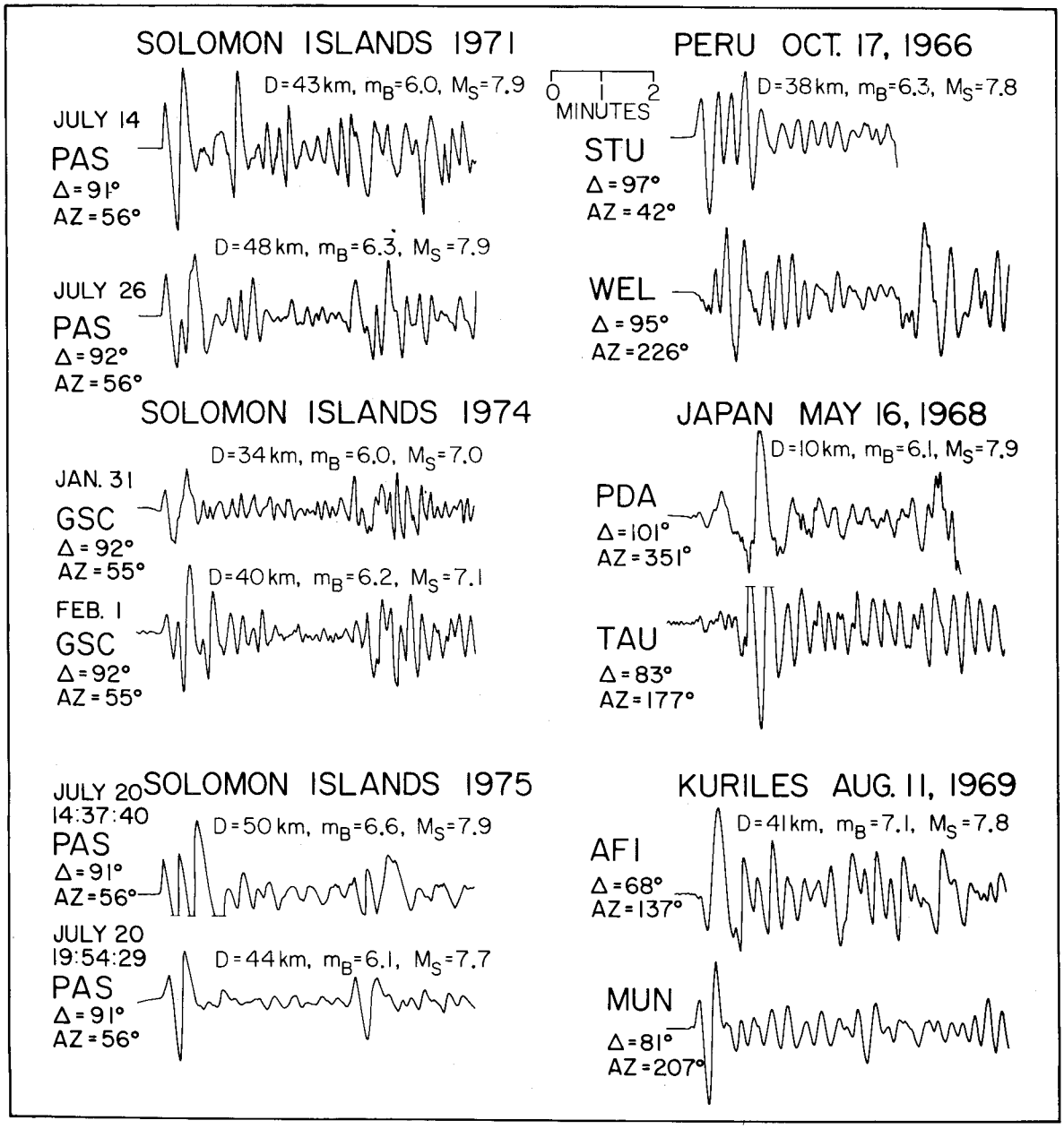


Fig. 13. Long-period vertical component body wave arrivals for the Solomon Islands events and for other circum-Pacific thrust events of comparable moment. Stations are chosen in loop directions of the P-wave radiation patterns. Relative amplitudes are not conserved, thus the 1974 doublet is relatively enhanced.

$\tau = 5$ s and $t_c = 9$ s. The width of the initial half cycle is the most sensitive to $t_c$, and this is the basic feature we want to model. Clearly, however, this simple source is adequate to meet the full pulse form of the event. All of the stations at distances greater than 80° are in the loop direction of the P-wave and these are the most stable in wave form. The station LEM has some high-frequency noise which we attribute to

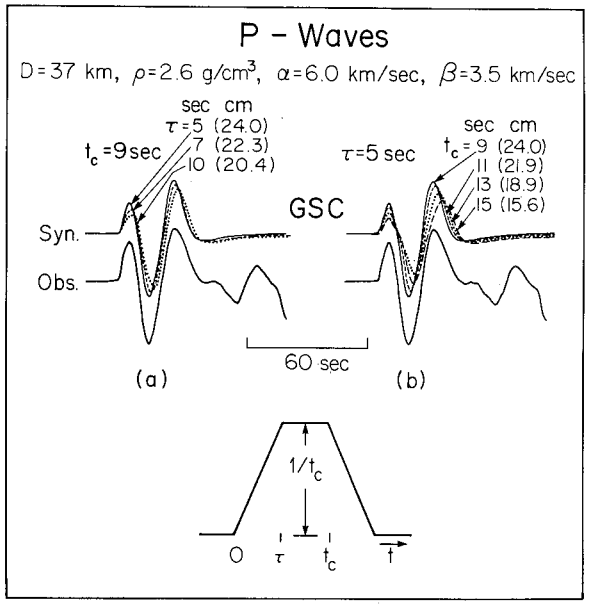


Fig. 14. Trapezoid function used in the synthesis and the change of synthetic P-wave form for GSC for variation of (a) rise time $\tau$, and (b) rupture time $t_c$. The numbers in parentheses indicate the peak-to-peak amplitude on a standard WWSSN long-period seismogram (X1500) for a source moment of $10^{27}$ dyne cm.

receiver structure or path effects as this complexity was not observed at other stations. Both MUN and ANP go off-scale on the second upswing but the initial pulse width is consistent with the synthetics. The moments are taken from comparison of amplitudes of the observed data and the synthetics generated for a moment of $1.0 \cdot 10^{27}$ dyne cm. The average of the WWSSN data indicates a moment of $M_0 = 7 \cdot 10^{26}$ dyne cm, much smaller than the surface wave moment of $1.2 \cdot 10^{28}$ dyne cm. Inspection of Fig. 13 indicates that for this event a slightly smaller, but similar second rupture took place about one minute after the initial rupture. This again appears to be a rather distinct impulsive event, but a reliable time function for it could not be obtained due to contamination by the coda of the first rupture. The overall pulse width does indicate that the time function is similar to that of the first rupture. Given the quality of the body wave fit for the pulse width and wave form we are confident that we have a good estimate of the source time function for this event.

It was of particular interest to determine whether the July 26, 1971 event was of a similar moment and time function to the July 14 event. The only useable body wave record was that of the Pasadena instrument. For the mechanism found by the surface wave analysis this record is fortunately in the loop direction of the P-wave radiation pattern. Figure 16 shows the Pasadena record and a matched synthetic generated by a double source. The time functions for the two sources are $\tau_1 = 5$ s, $t_{c1} = 11$ s, and $\tau_2 = 4.0$ s,

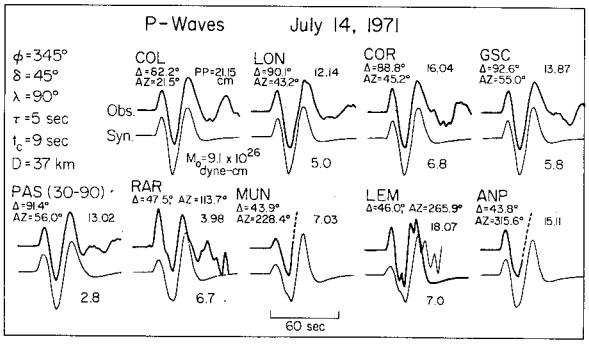


Fig. 15. Observed P-wave forms and matched synthetics for the July 14, 1971 event. PP denotes the peak-to-peak amplitude on the original seismograms. The moment $M_0$ is obtained by matching the amplitudes of the observed and synthetic records.

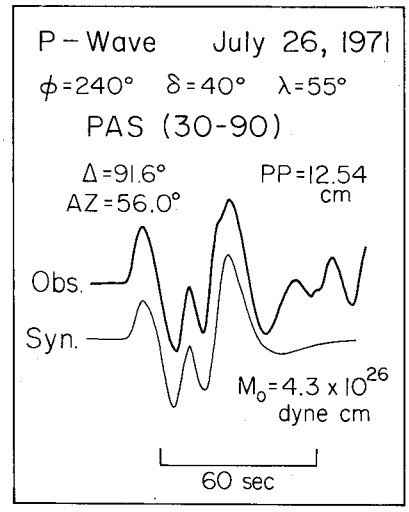


Fig. 16. Observed P-wave form and matched synthetic of the Pasadena Press–Ewing seismogram of the July 26, 1971 event. The source time function of the synthetic is discussed in the text.

$t_{c2}$ = 7.0 s. The first event was placed at 43 km depth and the second occurred 18 s after the onset of the first event at 23 km depth. The second event's moment is 60% of the moment of the first. A combined moment of $4.3 \cdot 10^{26}$ dyne cm with an uncertainty factor of about 2 was obtained. Although this model is not unique, our basic interest was to bound the rupture time of the event, and a $t_c$ of 11 s seems reliable for at least the first event. Examination of diffracted P-waves from this event, which are subject to substantial pulse broadening, further supported an upper bound on $t_c$ of 11 s. It is interesting that there are again two similar ruptures recorded in the body wave arrival.

Owing to unfortunate timing of the first event of the 1975 sequence, with almost all of the P-waves recorded at United States stations being truncated at the end of the seismogram, we did not have enough good data to do a detailed study of this event. Azimuthal coverage indicates that a double source can match much of the data though a few azimuths seem to require a third source. The sources again appear to be of similar nature and size, as indicated in the Pasadena record (Fig. 13). A value of $t_c$ = 9 s for the first of these ruptures was found to be very consistent at all recorded azimuths. Given the complexity of the event and the lack of good record we satisfied ourselves with the initial pulse rupture time.

The second member of the 1975 doublet is much simpler in character and better recorded. Figure 17 shows a selection of the data and synthetics generated using the surface wave fault orientation and a depth of 25 km. There is a small precursory event of about one-fifth the moment of the main event occurring 4.5 s before the main pulse. We included this in a two source model so as not to misinterpret the initial pulse width. For modelling purposes the precursor was located at the same hypocenter as the main event. Stations at a distance of greater than 80°; LON, COR, and PAS, were slightly broadened with respect to those at lesser distances. This may be a manifestion of up-dip rupture propagation (toward the southwest), but such directivity is uncertain, and rather than attempt an overly sophisticated finite source model we generate synthetics allowing some variation in the time functions. It was found that the precursory time function for the distant stations was $\tau$ = 3.0 s, $t_c$ = 5.0 s whereas for the nearer stations

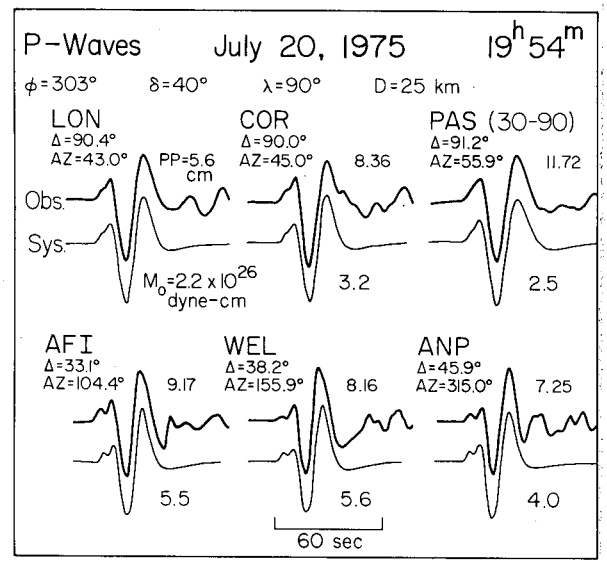


Fig. 17. Observed P-wave forms and matched synthetics for the $19^h54^m$ July 20, 1975 event. The source time functions of the synthetics are discussed in the text.

$\tau$ = 2.0 s, $t_c$ = 4.0 s. The time function for the main event, which is what we want most, was fitted at all azimuths with $\tau$ = 4.0 s and $t_c$ = 6.0 s. The slight discrepancy in the precursor may well be due to it having a slightly different mechanism than the main event. The average moment obtained was $3.2 \cdot 10^{26}$ dyne cm, and the good fit of the main event indicates that $t_c$ = 6.0 s is reliable for this earthquake. The $14^h37^m$ event apparently consists of two or three ruptures, and its resulting fault area may be two or three times larger than the $19^h54^m$ solitary source thus yielding the larger (surface wave) moment found for the first event.

We did not attempt to model in detail the 1974 events because the body waves are much smaller, and somewhat surprisingly in the case of February 1, 1974, fairly complex. A rupture time of $t_c$ = 9 s was suggested by models of the pulse width in the case of the January 31, 1974 earthquake. There is some question about this because the wave forms are apparently caused by interaction of two sources of slightly different mechanism, thus we concerned ourselves only with the four larger, more significant events.

Given the time functions of the events we approximated the source dimensions of the body wave radia-

tion. We assumed a typical rupture velocity of 3 km $s^{-1}$. For the July 14, 1971 event, $t_c = 9$ s, yielding fault lengths of $L_u \sim 27$ km and $L_b \sim 54$ km for unilateral and bilateral faulting respectively. There is no strong evidence as to which type of faulting is more realistic. For the July 26 event $t_c = 11$ s giving $L_u \sim 33$ km and $L_b \sim 66$ km. For the first 1975 event with $t_c = 9$ s we get $L_u \sim 27$ km and $L_b \sim 54$ km while for the second event $t_c = 6$ s, giving $L_u \sim 18$ km, and $L_b \sim 36$ km. The source dimension estimates for both body waves and surface waves are tabulated in Table III. The source dimension differences are most apparent for the 1971 events, while the 1975 events results are less conclusive if bilateral faulting is assumed. The displacements and stress drops associated with the body waves are subject to a good deal of uncertainty. The most conservative estimates yield stress drops comparable to the surface wave results, and probably they could be several times greater, but to draw further conclusions about this is not warranted by the scant data. The important result of the body wave analysis is that relative to the areas which radiated the long-period surface waves the body waves were radiated from substantially smaller, isolated regions. The occurrence of one or two distinct impulsive ruptures in each event indicates that the zones of strong coupling that fail, producing the body waves, are distributed over the fault surface in discrete patches.

## 6. Discussion

### *6.1. Tectonic framework*

Figure 1 summarizes the essential features of the Solomon Islands tectonic region. The Indian–Pacific convergence direction and rate of 11 cm $yr^{-1}$ is an average value of those given by Le Pichon (1968), Chase (1971), and Minster et al. (1974). The direction of convergence varies along the trench and is sensitive to the exact location of the Indian–Pacific pole of rotation, but is fairly well constrained at around N68E (Curtis, 1973a; Kraus, 1973). Previous authors have suggested the existence of several small plates, including the Solomon Sea plate, the Bismark plate lying northwest of New Britain, and possibly a third small plate north of the Bismark Sea seismic zone indicated in Fig. 1 (Denham, 1969; Johnson and Molnar, 1972; Curtis, 1973b; Kraus, 1973). These complexities have mainly been inferred from the seismicity and first-motion mechanisms. The best documented sub-plate appears to be the Bismark plate, bounded on the north by the Bismark Sea seismic zone, on the southwest by the complex convergent zone along northern New Guinea, and on the southeast by the New Britain trench. The existence of this platelet is supported by bathymetric, magnetic, volcanic, seismic reflection, and seismicity data (Johnson and Molnar, 1972; Connelly, 1974, 1976; Ripper, 1975). Numerous left-lateral strike slip mechanisms defining the Bismark Sea seismic zone are in the literature, and this feature is indicated in Fig. 1 (Johnson and Molnar, 1972; Curtis, 1973b; Kraus, 1973). This seismic lineation enters the Solomon Sea tangentially to the Solomon trench at the convergent region of the Solomon and New Britain trenches. Thus, this source region of the 1971 doublet is a triple junction.

Several authors have proposed the existence of spreading at a rate of 2.25 cm $yr^{-1}$ along the Woodlark Ridge (Milsom, 1970; MacDonald et al., 1973; Luyendyk et al., 1973) based on magnetic anomaly data and heat flow, but no focal mechanisms are published definitely supporting this. The presence of the Woodlark Ridge may be related to the shallowing out of the Solomon trench in the central Solomon Islands. If the Woodlark Ridge is indeed a plate boundary, the Solomon Sea may be a small plate itself. The southwestern termination of this plate would be along the Papuan ultramafic belt, a region of extensive faulting but relatively sparse present day seismicity. Johnson and Molnar (1972) analyzed numerous first-motion mechanisms and concluded that the thrusting in the Solomon trench is predomi-

TABLE III

Source dimension estimates

| Event | Body waves | | Aftershock zone | |
|---|---|---|---|---|
| | Unilateral (km) | Bilateral (km) | Length (km) | Width (km) |
| July 14, 1971 | 27 | 54 | 200 | 70 |
| July 26, 1971 | 33 | 66 | 300 | 70 |
| July 20, 1975 | 27 | 54 | 135 | 90 |
| July 20, 1975 | 18 | 36 | | |

nantly in a direction N34°E which would indicate that the Solomon Sea is acting somewhat independently of the global Indian–Pacific convergence. South of 10°S the thrusting is apparently consistent with the Pacific–Indian convergence vector. An alternate proposal has been raised by Pascal (1978) who feels that plate tectonics theory does not apply rigorously to the area. He employs a slip-line field theory for a geodynamical model which does not require a separate Solomon plate. Even with a separate Solomon plate moving in a direction of N34°E it is difficult to explain the convergence in the New Britain trench, the area with the highest seismic activity in the region. One of the poorest known quantities in triple junction vector analysis of this region has been the convergence rate in the New Britain trench (Curtis, 1973a; Kraus, 1973).

Our results provide the first quantification of the Solomon Island tectonic framework beyond what has been determined through seismicity studies. Examination of Fig. 3 shows that in general our results are consistent with the previous tectonic models. The July 26, 1971 event indicates underthrusting of the Solomon plate in the New Britain trench on a fault plane striking along the trend of the trench. The thrust direction of the event is N18°E, which is consistent with the gross northeastward movement of the Indian plate relative to the Pacific plate. Even if the Solomon plate is somewhat uncoupled from the Indian plate it must still accommodate the northward movement of the larger plate. It should be noted that in this region the movement of the Indian plate is the basic controlling feature of the tectonics, for it underthrusts the westward moving Pacific plate. The New Britain fault plane orientation at N60°E is consistent with the results of Johnson and Molnar (1972) and Kraus (1973) who have given an average fault plane orientation of N73°E in the southwest end of the trench and N63°E in the central portion. The triple junction analyses performed by Kraus (1973) and Curtis (1973a) predict very large convergence rates in this trench of 9.2–12.4 cm $yr^{-1}$.

In order to obtain an estimate of the seismic convergence rate we investigated the historical record of great earthquakes in the region. All the events with $M_S \geq 7.5$ are shown in Fig. 18, where we have divided the region into three areas, the New Britain trench, the Northwest Solomon trench along Bougainville,

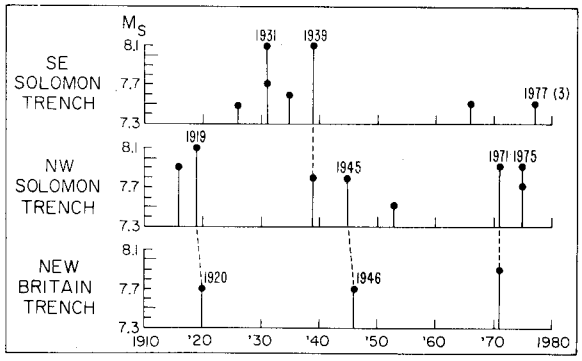


Fig. 18. Earthquakes of $M_S \geq 7.5$ in various portions of the Solomon Islands region. The Solomon trench is divided into regions northwest and southeast of the Woodlark Ridge. Dotted lines connect events inferred to be of doublet nature.

and the Southeast Solomon trench along Guadalcanal, around 10°S. The lower two rows include the region studied. Note that an approximately 25-year recurrence interval in both trenches is indicated. Also note the apparent occurrence of doublet sequences in 1919–1920 and 1945–1946. In both cases it appears as though a great earthquake in the Solomon trench triggered an event in the New Britain trench, though there is some uncertainty in the early locations. The time separation for these events is several months, somewhat longer than the 12 day separation of the 1971 sequence, however, the doublet nature seems to be repeated. The trench along Guadalcanal experiences somewhat similar events, including the 1931, 1939, and 1977 doublets and triplets, despite being separated from the northwestern trench. From this it appears that the doublet nature is a true characteristic of the Solomon Islands region. Large single events appear scarce relative to the paired events. Utilizing a recurrence interval of 25 years we obtained from the July 26, 1971 displacement of 1.3 m, a convergence rate of 5 cm $yr^{-1}$ as indicated in Fig. 1, though this is not purely in the direction perpendicular to the trench. This is a substantial rate, allowing much of the convergence in the New Britain trench to be accommodated seismically.

Consideration of the five mechanisms in the Solomon trench indicates that the convergence direction is roughly perpendicular to the orientation of the trench. Thrusting south of Bougainville is directed from N32°E to N39°E, and in the northern vicinity of the triple junction the convergence is about N65°E

to N110°E. The latter value is somewhat uncertain due to scatter in the data of the July 14, 1971 event, but is consistent with the Indian–Pacific convergence direction. Since the 1971 event is an order of magnitude larger than the others it is most representative of the regional motion. From the 1971 displacement of 1.3 m we get a convergence rate of 5 cm $yr^{-1}$. This is a substantial portion of the predicted total Indian–Pacific convergence rate of 11 cm $yr^{-1}$, indicating that much of the convergence in this trench is also taken up seismically. The other mechanisms, though from smaller events, indicate that along the length of the trench the convergence is rather uniform in a direction more like N35°E. This is consistent with Johnson and Molnar's (1972) results and supports their contention that to some degree the Solomon slab is acting independently of the gross Indian–Pacific convergence. The apparent discrepancy in convergence direction in this trench may be associated with the location of the July 14 event at the triple junction, or alternatively with the sub-plate nature of the Solomon plate as discussed below.

There is no indication of a large right lateral component in these mechanisms which might be expected if the Woodlark Ridge was producing significant spreading toward the northwest. Thus it appears that the convergence in the New Britain trench cannot be attributed to northwestward motion of the Solomon slab. We consider this trench to be the result of clockwise rotation of the Bismark plate, pushed from the southwest border along New Guinea and rotating over the Solomon Sea slab. The Solomon Sea slab may be partially decoupled from the Indian plate, moving in a more northerly direction, with spreading in the Woodlark Ridge accommodating this divergence, but as the 1971 sequence shows , the Solomon slab behaves in the largest events as though it were affixed to the Indian plate. This interpretation is supported by the result of Luyendyk et al. (1973) that shows that spreading of the Woodlark Ridge is only occurring in the northeast and has stopped along the southwestern part of the ridge. This state of only partial decoupling also explains the lack of a well-defined plate boundary along the Papua Peninsula, as here the Indian and Solomon plates are joined. This interpretation keeps the tectonic situation in a simple consistent framework which explains the observed seismicity and geometry.

### *6.2. Doublet mechanism*

Having determined the mechanisms, moments, and displacements of the individual members of each doublet, and having a unified overview of the tectonics characterizing this region, we now attempt to synthesize a simple model to explain the doublet earthquake behavior observed. Pertinent observations include the fact that the convergence rate in the Solomon trench is quite high, about 11 cm $yr^{-1}$, and that the repeated occurrence of doublets indicates that triggering of adjacent events operates efficiently here. Triggering also occurs around the trench junction which indicates continuity of the subducting slab around this curvature, at least at shallow depths. A substantial amount of the convergence is accommodated by seismic slip, which indicates strong mechanical coupling between the Solomon plate and the Ontong–Java Plateau which is being underthrust. The earthquake rupture dimensions in this region are on the order of a few hundred kilometers. The width of the contact zone cannot be determined directly, but it is apparent that at depths >100 km the Solomon slab is one of the steepest dipping slabs in the circum-Pacific zones (Denham, 1969; Isacks and Molnar, 1971; Curtis, 1973b; Uyeda and Kanamori, 1979). This argues for a relatively narrow contact zone at shallow depths, as is consistent with the observed width of aftershock zones and seismicity. Of great importance is the fact that the body wave analysis indicates that the area from which the body waves are radiated in these doublets is about an order of magnitude less than the total area radiating the surface waves.

A simplified asperity model is proposed to explain the basic features observed in this study and to provide a plausible model of the stress distribution on the fault plane. As demonstrated in Fig. 13, the body waves from the larger Solomon Islands earthquakes (events in 1971 and 1975) are impulsive, with very sharp onsets, while the body waves of the events from other subduction zones are rather complex, either starting with small precursory events (1968 Japan, 1969 Kurile) or containing a large number of smaller events following the first event (1966 Peru). This observation suggests that the stress distribution on the contact zone in the Solomon Islands is characterized by discrete high-stress regions (asperities) of

about the same size. In contrast, the size of asperities in other subduction zones is more variable, producing more complex events. Failure of one of the asperities would cause an increase in stress on the adjacent asperities. In the Solomon Islands region, where the asperities are large and of similar size, these incremental stresses are large enough to trigger failure of an adjacent asperity, producing two distinct but similar events in a sequence (Fig. 19). In other regions, where the stress distribution is inferred to be more heterogeneous, numerous small and intermediate size asperities must fail along with the larger ones, producing very complex events.

This difference in the distribution of asperities would be reflected in the pattern of foreshock and aftershock activity. If the asperities are more homogeneous in size, as in the Solomon Island region, one would expect fewer foreshocks and aftershocks. Although quantitative comparison of the nature of foreshock and aftershock activity between the Solomon Islands region and other regions is very difficult due to variations in detection thresholds and incomplete catalogues, inspection of the ISC Bulletin does suggest that the Solomon Islands earthquakes have relatively few foreshocks and aftershocks, particularly for these sequences of two large events. The 1974 doublet is the only sequence with immediate foreshocks, of which there are only two. The Solomon trench events typically have 24–27 aftershocks listed in the ISC Bulletin of $m_b \geqslant 4.5$ within the first 24 hours after the sequences. In contrast, the single 1968 Japan event was followed by 46 aftershocks, and the 1969 Kurile event was followed by 67 aftershocks, of $m_b \geqslant 4.5$ within 24 hours. The Kurile event also had seven foreshocks within 30 minutes prior to the main event. The July 26, 1971 event in the New Britain trench had significantly more aftershocks than the Solomon trench events. The distinct nature of the New Britain trench can be attributed to its unusual tectonic configuration, as it accommodates the northward movement of the Solomon slab as well as the eastward rotation of the Bismark plate.

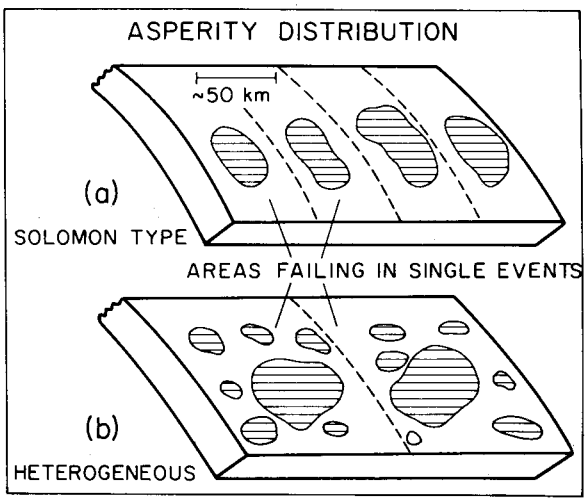


Fig. 19. Asperity model representation of coupling on the subducting slab. The Solomon Islands region has a uniform distribution of discrete, comparable size zones of coupling. Other areas such as Japan and the Kurile Islands have a more heterogeneous stress distribution.

Present understanding of earthquake failure process and stress propagation is insufficient to allow a dynamic analysis of the doublet phenomena. The time interval between individual members of these doublets ranges from several hours to 12 days, and each member typically has two or more impulsive events, separated by 10–60 s (Fig. 13). The factors controlling these rates are most likely to be the rheological properties and/or lateral segmentation of the contact zone (Mogi, 1969).

The principal factors governing the stress distribution found in the Solomon Islands region are probably the rapid convergence rate and the presence of the thick Ontong–Java Plateau. The rapid convergence rate produces the short recurrence time and rapid strain accumulation in the area. Underthrusting of the Solomon slab beneath the thick semi-continental Plateau accounts for the localized strong coupling in the contact zone, as the contact is with a thicker crust than normal for Island arcs. Little is known about the age and structure of the Solomon Sea slab, but it is believed to be of mid-Tertiary age (Karig, 1972), and may be older toward the northwest if the Woodlark spreading is significant. The fairly smooth Solomon Sea floor might contribute to the uniformity of asperity size in the Solomon trench, as more disrupted ocean floor would lead to greater heterogeneity of coupling, but at this point it is difficult to relate material properties to the nature of the stress distribution.

## 7. Conclusions

Detailed analysis of three earthquake doublets in the Solomon Islands has led to an improved understanding of the stress distribution and nature of convergence in this portion of the Indian–Pacific plate boundary. The doublets include the largest events in the region, and by constraining their mechanisms we have quantified the tectonic framework of the area. There is a high convergence rate in the Solomon trench, a substantial portion of which is accommodated seismically. A short recurrence interval of only 25 years is observed. Subduction in the Solomon trench appears to be fairly uniform with a thrust direction of N35°E, more northerly than the Indian–Pacific convergence direction of N68°E, which indicates some degree of independent behavior of the Solomon slab, however, in the great earthquakes of the region the convergence proves to be in a direction consistent with the Indian–Pacific convergence, thus the behavior of the Solomon slab is not wholly independent of the Indian plate. The junction of the New Britain and Solomon trenches appears to be a triple junction with the subducting slab being continuous between the trenches. Clockwise rotation of the Bismark plate onto the Solomon Sea accounts for the existence of the New Britain trench.

It was determined that the source dimensions of the body waves had lengths of 30–70 km, substantially smaller than the source dimensions of the surface waves with lengths of 100–300 km. Also, the body waves are unusually impulsive and simple for large subduction zone events. It appears that the stress distribution is characterized by a relatively homogeneous distribution of discrete high-stress zones along the fault contact. Failure of these discrete zones induces high, rapidly accumulated stress concentrations on adjacent areas leading to a second major failure and the doublet behavior. The characteristic separation of these asperities appears to be ~50–100 km. A result of this type of stress distribution is the high efficiency of seismic triggering relative to more heterogeneous stress distributions. The high convergence rate and the fact that the Solomon Sea slab is subducting under the thick Ontong–Java Plateau are believed to be principal features responsible for the inferred stress distribution.

## Acknowledgements

We would like to thank Gordon S. Stewart for helpful discussions and use of his equalization programs, and G. Pascal for providing a preprint. We also thank Gordon S. Stewart and John E. Ebel for critically reading the manuscript. This research was supported by a grant from the National Science Foundation (EAR78-11973) and by U.S. Geological Survey Contract (14-08-0001-17631). One of the authors, Thorne Lay, was supported by a National Science Foundation Graduate Fellowship. Contribution No. 3163, Division of Geological and Planetary Sciences, California Institute of Technology, Pasadena, California, 91125.

## References

Ben-Menahem, A., 1961. Radiation of seismic waves from finite moving sources. Bull. Seismol. Soc. Am., 51: 401–435.

Chase, C., 1971. Tectonic history of the Fiji Plateau. Bull. Geol. Soc. Am., 82: 3087–3109.

Coleman, P.J. and Packam, G.H., 1976. The Melanesian borderlands and India–Pacific plate boundary. Earth Sci. Rev., 12: 197–233.

Connelly, J.B., 1974. A structural interpretation of magnetometer and seismic profile records in the Bismark Sea, Melanesian Archipelago. J. Geol. Soc. Aust., 21: 459–469.

Connelly, J.B., 1976. Tectonic development of the Bismark Sea based on gravity and magnetic modelling. Geophys. J. R. Astron. Soc., 46: 23–40.

Curtis, J.W., 1973a. The spatial seismicity of Papua New Guinea and the Solomon Islands. J. Geol. Soc. Aust., 20: 1–20.

Curtis, J.W., 1973b. Plate tectonics and the Papua New Guinea–Solomon Islands region. J. Geol. Soc. Aust., 20: 21–36.

Denham, D., 1969. Distribution of earthquakes in the New Guinea–Solomon Islands region. J. Geophys. Res., 74: 4290–4299.

Dewey, J.F. and Bird, J.M., 1970. Mountain belts and the new global tectonics. J. Geophys. Res., 75: 2625–2647.

Fukao, Y. and Furumoto, M., 1975. Mechanism of large earthquakes along the eastern margin of the Japan Sea. Tectonophysics, 24: 247–266.

Furumoto, A.S., Webb, J.P., Odegard, M.E. and Gussong, D.M., 1976. Seismic studies on the Ontong–Java Plateau. Tectonophysics, 34: 71–90.

Isacks, B. and Molnar, O., 1971. Distribution of stresses in the descending lithosphere from a global survey of focal

mechanism solutions of mantle earthquakes. Rev. Geophys. Space Phys., 9: 103–174.
Johnson, T. and Molnar, P., 1972. Focal mechanisms and plate tectonics of the southwest Pacific. J. Geophys. Res., 77: 5000–5032.
Kanamori, H., 1970. Synthesis of long-period surface waves and its application to earthquake source studies, Kurile Islands earthquake of October 13, 1963. J. Geophys. Res., 75: 5011–5027.
Kanamori, H., 1972. Mechanism of tsunami earthquakes. Phys. Earth Planet. Inter., 6: 346–359.
Kanamori, H. and Cipar, J.J., 1974. Focal process of the great Chilean earthquake May 22, 1960. Phys. Earth Planet. Inter., 9: 128–136.
Kanamori, H. and Stewart, G.S., 1976. Mode of strain release along the Gibbs fracture zone, Mid-Atlantic Ridge. Phys. Earth Planet. Inter., 11: 312–332.
Kanamori, H. and Stewart, G.S., 1978. Seismological aspects of the Guatemala earthquake of February 4, 1976. J. Geophys. Res., 83: 3427–3434.
Kanamori, H. and Stewart, G.S., 1979. A slow earthquake. Phys. Earth Planet. Inter., 18: 167–175.
Karig, D.E., 1972. Remnant arcs. Bull. Geol. Soc. Am., 83: 1057–1068.
Kraus, D.C., 1973. Crustal plates of the Bismark and Solomon Seas. In: R. Frazer (Editor), Oceanography of the South Pacific. N. Z. Nat. Comm. UNESCO, Wellinton, pp. 271–280.
Langston, C.A. and Helmberger, D.V., 1975. A procedure for modelling shallow dislocation sources. Geophys. J. R. Astron. Soc., 42: 117–130.
Le Pichon, X., 1968. Sea-floor spreading and continental drift. J. Geophys. Res., 78: 2537–2546.
Luyendyk, B.P., MacDonald, K.C. and Byran, W.B., 1973. Rifting history of the Woodlark Basin in the Southwest Pacific. Bull. Geol. Soc. Am., 84: 1125–1131.
MacDonald, K., Luyendyk, B. and von Herzen, R.P., 1973. Heat flow and plate boundaries in Melanesia. J. Geophys. Res., 78: 2537–2546.
Milson, J.S., 1970. Woodlark Basin, a minor centre of sea-floor spreading in Melanesia. J. Geophys. Res., 75: 7335–7339.
Minster, J.B., Jordan, T.H., Molnar, P. and Haines, E., 1974. Numerical modelling of instantaneous plate tectonics. Geophys. J. R. Astron. Soc., 36: 541–576.
Mogi, K., 1969. Relationship between the occurrence of great earthquakes and tectonic structure. Bull. Earthquake Res. Inst., 47: 429–451.
Nagamune, T., 1977. Time characteristics of crustal deformation of the Yunnan earthquake of May 29, 1976, as inferred from tilt recording. J. Phys. Earth, 25: 209–218.
Packham, G.H., 1973. A speculative Phanerozoic history of the Southwest Pacific. In: P.J. Coleman (Editor), The Western Pacific; Island Arcs, Marginal Seas, Geochemistry. University of Western Australia, Perth, pp. 369–388.
Pascal, G., 1979. Seismotectonics of the Papua New Guinea–Solomon Islands region. Tectonophysics, 57: 7–34.
Ripper, I.D., 1975. Seismicity and earthquake focal mechanisms in the New Guinea–Solomon Islands region. Bull. Aust. Soc. Explor. Geophys., 6: 80–81.
Sacks, I.S., Suyehiro., S. Linde, A.T. and Snoke, J.A., 1978. Slow earthquakes and stress redistribution. Nature (London), 275: 599–602.
Santo, T., 1970. Regional study of the characteristic seismicity of the world. Part IV. New Britain Island region. Bull. Earthquake Res. Inst., 48: 127–143.
Shimazaki, K. and Geller, R. J., 1977. Source process of the Kurile Islands tsunami earthquake of June 10, 1975. Eos, 58: 446.
Uyeda, S. and Kanamori, H., 1979. Back-arc opening and the mode of subduction. J. Geophys. Res., 84: 1049–1061.
Wyss, M. and Brune, J.N., 1967. The Alaska earthquake of 28 March 1964: a complex multiple rupture. Bull. Seismol. Soc. Am., 57: 1017–1023.